

BRIEF REPORT

Distance of Lipid Core–Rich Plaques From the Ostium by NIRS in Nonculprit Coronary Arteries

Salvatore Brugaletta, MD,‡ Hector M. Garcia-Garcia, MD, PhD,*†
Patrick W. Serruys, MD, PhD,* Josep Gomez-Lara, MD,* Sanneke de Boer, MD,*
Jurgen Ligthart, BSc,* Karen Witberg, RN,* Cihan Simsek, MD,*
Robert-Jan van Geuns, MD, PhD,* Carl Schultz, MD, PhD,*
Henricus J. Duckers, MD, PhD,* Nicolas van Mieghem, MD,* Peter de Jaegere, MD, PhD,*
Sean P. Madden, PhD,§ James E. Muller, MD,§ Antonius F. W. van der Steen, PhD,*
Eric Boersma, PhD,* Wim J. van der Giessen, MD, PhD,* Felix Zijlstra, MD, PhD,*
Evelyn Regar, MD, PhD*

Rotterdam, the Netherlands; Barcelona, Spain; and Burlington, Massachusetts

Previous angiographic studies have failed to identify those quiescent plaques prone to progress or rupture, as most of them are non–flow limiting (1). Plaque composition was demonstrated not to be uniformly distributed along each coronary artery, and in patients with ST-segment elevation acute myocardial infarction, culprit lesions tend to cluster within the proximal third of each coronary artery (2,3). Intravascular ultrasound (IVUS) virtual histology (VH), has demonstrated higher necrotic core content of coronary plaque close to the coronary ostium compared with the distal counterpart (4).

Recently, a novel catheter-based intracoronary imaging system, based on near-infrared spectroscopy (NIRS), has been developed for the specific purpose of identification of lipid core plaque (LCP) (5). A weak correlation has been demonstrated between NIRS and VH findings for detecting lipid or necrotic core–rich plaques (6). The aim of the present study is to assess LCP distribution in nonculprit coronary arteries using NIRS.

Sixty-eight consecutive patients, in whom a nonculprit, nontreated vessel was judged suitable for a

safe NIRS pullback of 50 mm or more in length were enrolled (Table 1). The inclusion/exclusion criteria have been previously published (6). The study was conducted under the guidance of the institutional review board, and written informed consent was required.

Each region of interest (ROI), starting from the coronary ostium, was divided into 10-mm segments, corresponding to 5 block chemograms by NIRS (5). For each ROI and 10-mm segment, the mean value of the block chemogram and the number of LCP (absolute and relative) were calculated. A LCP was considered to be present if at least 1 2-mm block chemogram had a strong positive reading as signaled by yellow color, as previously described (5). The presence of at least 3 non–yellow block chemograms in-between 2 LCP was required in order to consider them as 2 independent LCP.

Categorical variables are presented using frequencies and percentages, continuous variables with mean and standard deviations or median and ranges, according to their distribution. A generalized estimating equations approach was used to compensate for any potential cluster effect of multiple lesions in the same patient. Block chemogram values per 10-mm segment are presented as least-square means with 95% confidence intervals (CI). A univariate (including age, sex, dyslipidemia, acute coronary syndrome at presentation, coronary vessel [right coronary artery (RCA) vs. the others], and distance from the ostium [segment 1 vs. the others]) and logistic generalized estimating equations approach (including all variables with a p value ≤ 0.1

From the *Thoraxcenter, Erasmus Medical Center, Rotterdam, the Netherlands; †Cardialysis BV, Rotterdam, the Netherlands; the ‡Department of Cardiology, Thorax Institute, Hospital Clinic, Barcelona, Spain; and §InfraReDx, Inc., Burlington, Massachusetts. Dr. Ligthart has a procor contract (IVUS) with Boston Scientific and teaching contracts with Volcano Inc. and St. Jude Medical. Drs. Madden and Muller are current employees of InfraReDx, Inc. Dr. Madden holds ownership interest in InfraReDx, Inc. All other authors have reported that they have no relationships relevant to the contents of this paper to disclose.

Manuscript received August 16, 2011; revised manuscript received September 21, 2011; accepted September 22, 2011.

Table 1. Baseline Characteristics of the Patients/Vessels Included (n = 68)	
Age, yrs	62 ± 10
Sex, male	53 (78)
Clinical history	
Dyslipidemia	41 (60)
Hypertension	40 (58)
Diabetes mellitus	15 (22)
Current smoker	39 (57)
Prior MI	29 (42)
Prior PCI	29 (42)
Prior coronary artery bypass graft	4 (5)
Clinical presentation	
Stable angina	32 (47)
Acute coronary syndromes	36 (53)
Vessel investigated by NIRS	
LAD	22 (32)
LCX	30 (44)
RCA	16 (24)
IVUS analysis	
Lumen volume, mm ³	273.39 ± 157.17
Vessel volume, mm ³	470.64 ± 289.91
Plaque burden, %	38.77 ± 12.75
Values are n (%) or mean ± SD. IVUS = intravascular ultrasound; LAD = left anterior descending artery; LCX = left circumflex artery; MI = myocardial infarction; NIRS = near-infrared spectroscopy; PCI = percutaneous coronary interventions; RCA = right coronary artery.	

at univariate analysis) were applied to estimate the independent predictors of LCP. A 2-sided p value <0.05 indicated statistical significance. Statistical analyses were performed using SPSS 17.0 software (SPSS Inc., Chicago, Illinois).

Overall, the length of the ROI was 58.0 ± 4.3 mm, with a total of 392 10-mm segments (56 and 67

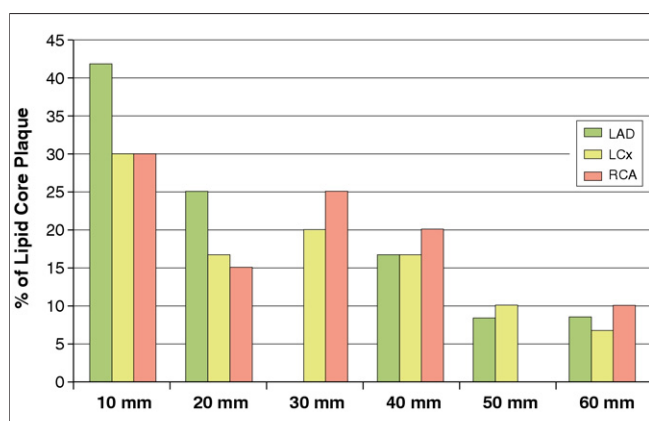


Figure 1. Percentage of LCP in the six 10-mm Segments From the Ostium in the 3 Coronary Arteries

Values of p for the distribution are 0.042 for the left anterior descending coronary artery (LAD), 0.029 for the left circumflex coronary artery (LCX), and 0.041 for the right coronary artery (RCA). LCP = lipid core plaque.

patients with 6 and 5 10-mm segments available, respectively) and 1,903 block chemograms. Per ROI, the block chemogram value and the IVUS plaque burden were 0.33 ± 0.20% and 38.77 ± 12.75%, respectively. A total of 62 LCP were identified.

Block chemogram values were differently distributed between the 3 coronary arteries (left anterior descending coronary artery [LAD]: 0.24 ± 0.15 vs. left circumflex coronary artery [LCX]: 0.35 ± 0.19 vs. RCA: 0.42 ± 0.23, p = 0.014). Forty-eight percent of the LCP were found in the LCX, 32% in the RCA, and the remaining 20% in the LAD (p = 0.107). At IVUS analysis, plaque burden tended to be higher in the RCA than in the LCX or LAD (45.17 ± 14.60% vs. 38.36 ± 10.19% vs. 35.76 ± 13.71%, p = 0.117).

The block chemogram value stratified per 10-mm segment showed a significantly different distribution in the 60 mm analyzed from the ostium (1st segment: 0.41, 95% CI: [0.34 to 0.48]; 2nd: 0.36, 95% CI: [0.29 to 0.42]; 3rd: 0.37, 95% CI: [0.30 to 0.43]; 4th: 0.32, 95% CI: [0.26 to 0.39]; 5th: 0.26, 95% CI: [0.20 to 0.33]; and 6th: 0.26, 95% CI: [0.19 to 0.33]; p = 0.011). The LCP were also differently distributed between the various segments analyzed, clustering close to the ostium (32.2% in the first 10-mm segment; 17.7% in the 2nd, 3rd, and 4th segments; 6.4% in the 5th segment; and 8.0% in the 6th segment; p < 0.001). The plaque burden did not show a significantly different distribution between the same 10-mm segments (p = 0.784).

Although the block chemogram values were confirmed to be heterogeneously distributed in the LAD and in the LCX, with the highest values closest to the ostium (LAD, p < 0.001. LCX, p = 0.001), in the RCA they were more homogeneously distributed (p = 0.155). The distribution of LCP within the 3 coronary arteries reflects this finding (Figs. 1 and 2). The distribution of plaque burden stratified per 10-mm segment was not statistically different within each coronary artery (data not shown). Distance from the ostium was the only independent predictor of LCP (odds ratio: 0.37 95% CI: [0.20 to 0.69]; p = 0.002).

The present analysis utilizes NIRS to study the longitudinal distribution of LCP in vivo. It has been demonstrated that the ability of this technique in detecting lipid/necrotic core plaques is weakly correlated with VH (6). Nevertheless, our analysis showed that the nonhomogeneity of LCP distribution along the coronary arteries is in agreement with prior anatomopathological, angiographic, and IVUS observations (2-4). In particular, LCP distribution along

the vessel wall is independently affected by the distance from the coronary ostium, resembling the distribution of the culprit lesions in ST-segment elevation myocardial infarction patients. Presence of tortuosity or frequent branching close to the ostium may explain this finding: significant variation in shear stress has been indeed demonstrated at the level of bifurcations or bending, and low shear stress may be implicated in the migration of lipids and monocytes into the vessel wall, processes that could accelerate the progression of an atherosclerotic lesion toward a vulnerable plaque (7).

Of note is that the distribution of block chemogram values and of LCP was different between the 3 coronary arteries: in particular, LCP were mainly located in proximal portions of the LAD and LCX, and were more uniformly distributed in the RCA (Figs. 1 and 2). These findings are also in line with previous anatomopathological studies (2,3).

Our analysis may have important clinical implications, especially for the design and interpretation of future studies. Of note is that LCP distribution is not related to IVUS plaque burden distribution so that NIRS may provide some clues for detecting in vivo vulnerable plaques, which lead to coronary event prediction. Moreover, it is known that percutaneous treatment of LCP can cause embolization of material with periprocedural myocardial infarction (8). For this reason, percutaneous treatment of plaques located close to the LAD or LCX ostia may represent PCI at risk of embolization, whose treatment can benefit from strategies preventing embolization.

Study limitations. The small sample size is a possible limitation of our analysis, although it represents so

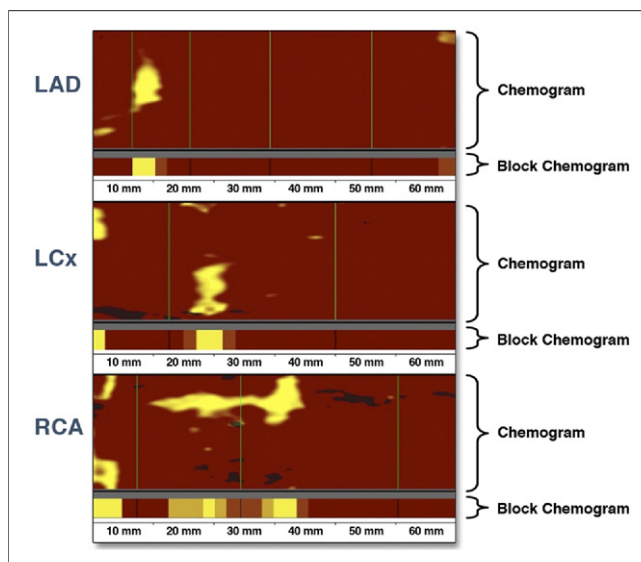


Figure 2. Examples of Distribution of LCP

The presence of LCP is indicated as yellow, 2-mm-long block chemograms, in the 3 coronary arteries, from the coronary ostium (left) up to 60 mm distally. Abbreviations as in Figure 1.

far the largest cohort of patients who have received a NIRS analysis. Of note is that our study is not a 3-vessel imaging analysis and does not include in the analysis the vessel containing the culprit lesion.

Acknowledgments

This paper is dedicated to Professor Dr. W. J. van der Giessen, who sadly passed away in June 2011.

Reprint requests and correspondence: Dr. P. W. Serruys, Interventional Cardiology Department, Erasmus Medical Center, Thoraxcenter, 's Gravendijkwal 230, 3015 CE, Rotterdam, the Netherlands. E-mail: p.w.j.serruys@erasmusmc.nl.

REFERENCES

1. Topol EJ, Nissen SE. Our preoccupation with coronary luminology. The dissociation between clinical and angiographic findings in ischemic heart disease. *Circulation* 1995;92:2333-42.
2. Wang JC, Normand SL, Mauri L, Kuntz RE. Coronary artery spatial distribution of acute myocardial infarction occlusions. *Circulation* 2004; 110:278-84.
3. Cheruvu PK, Finn AV, Gardner C, et al. Frequency and distribution of thin-cap fibroatheroma and ruptured plaques in human coronary arteries: a pathologic study. *J Am Coll Cardiol* 2007; 50:940-9.
4. Valgimigli M, Rodriguez-Granillo GA, Garcia-Garcia HM, et al. Distance from the ostium as an independent determinant of coronary plaque composition in vivo: an intravascular ultrasound study based radiofrequency data analysis in humans. *Eur Heart J* 2006;27:655-63.
5. Waxman S, Dixon SR, L'Allier P, et al. In vivo validation of a catheter-based near-infrared spectroscopy system for detection of lipid core coronary plaques: initial results of the SPECTACL study. *J Am Coll Cardiol Img* 2009;2: 858-68.
6. Brugaletta S, Garcia-Garcia HM, Serruys PW, et al. NIRS and IVUS for characterization of atherosclerosis in patients undergoing coronary angiography. *J Am Coll Cardiol Img* 2011;4: 647-55.
7. Cunningham KS, Gotlieb AI. The role of shear stress in the pathogenesis of atherosclerosis. *Lab Invest* 2005; 85:9-23.
8. Schultz CJ, Serruys PW, van der Ent M, et al. First-in-man clinical use of combined near-infrared spectroscopy and intravascular ultrasound: a potential key to predict distal embolization and no-reflow? *J Am Coll Cardiol* 2010;56:314.

Key Words: atherosclerosis ■ lipid-core plaques ■ near-infrared spectroscopy.